Williams and Bjerknes model with growth limitation

S. C. Ferreira Junior *

Departamento de Física, Instituto de Ciências Exatas, Universidade Federal de Minas Gerais, CP 702, 30161-970, Belo Horizonte, MG, Brazil

Abstract

Williams and Bjerknes proposed a simple stochastic growth model to describe the tumor growth in the basal layer of an epithelium. In this work we generalize this model by including the possibility of saturation in the tumor growth as it is clinically observed. The time evolution of the average number of tumor cells and its variance for both the original and extended models are studied by analytical methods and numerical simulations. The generated growth patterns can be compact, connected or disconnected depending on the model parameters used, and their geometrical properties are characterized through the gyration radius, the number of interfacial cells and the density of empty sites inside the patterns.

Key words: Tumor growth, Stochastic process, Computer simulations
PACS: 87.10+e, 02.50.Ey, 87.16.Ac

1 Introduction

The population dynamics, including the growth of normal and tumor cells, is a traditional problem investigated in Physics and Biology [1]. In their original work, Williams and Bjerknes [2] built a model (WB model) to describe the tumor growth in the basal layer of an epithelium. In their model, one phase (the tumor cells) grows faster than the other (normal cells) by a factor κ, which represents the carcinogenic advantage. This model exhibits two distinct behaviors: unrestricted growth ($\kappa > 1$) and complete regression of the tumor ($\kappa \leq 1$). In the special case $\kappa = 1$ the tumor always disappears due to the fluctuations. It is worthwhile to mention that the WB model can also

* Corresponding author.
Email address: silviojr@fisica.ufmg.br (S. C. Ferreira Junior).

be applied to describe the growth of many systems involving two competing phases. Using an adequate time step, the WB model can be interpreted as a '*birth and death*' process [3] with constant division and death rates. Thus, all the well known results for stochastic processes can be used to understand this model.

However, real tumors exhibit, in addition to the two distinct behaviors previously described, a quiescent state in which the tumor size remains constant for a long time [4]. The underlying aspects of tumoral biodynamic diversity involve a complex set of biochemical processes and environmental constraints such as local nutrient availability, mechanical stress, immune response, etc. [4]. Numerous models of cancer growth have been recently proposed in order to describe the tumor progression, providing auxiliary tools for cancer diagnosis and therapy [5].

In this paper, we are proposing a generalization of the WB model in which the division and death rates of tumor cells depend on their total number. Specifically, the probability of cell division decreases whereas the cell death probability increases as the number of cancer cells increases. The paper is organized as follows. In section 2, the original and the extended WB models are defined. Sections 3 and 4 are dedicated to the analytical study of both discrete and continuous time versions of these models. In section 5, the geometrical properties of the growth patterns generated by the extended model are characterized through computer simulations. Finally, some conclusions are drawn in section 6.

2 The extended Williams and Bjerknes models

In the original WB model [2] the tissue is represented by a two-dimensional lattice where occupied sites represent tumor and empty sites normal cells. All the sites are initially empty, except the center of the lattice, since the tumor grows from a single malignant cell, in agreement with the theory of clonal origin of cancer [6]. The interfacial cells are defined as those that have one or more nearest-neighbor sites of the opposite type. The growth rule is very simple: one of the bonds between two opposite cell types is chosen at random with equal probability; the normal cell of this chosen bond is replaced by a tumor cell, with probability g, or the tumor cell is replaced by a normal one, with the complementary probability $r = 1 - g$. In terms of the carcinogenic advantage κ, these probabilities can be written as:

$$g = \frac{\kappa}{\kappa + 1} \tag{1}$$

and

$$r = \frac{1}{\kappa + 1}. \tag{2}$$

The limit $\kappa = \infty$ corresponds to the Eden model [7], more specifically, the Eden model type B according to the definitions given by Vicsek [8].

There are many variations of the WB model [9], but we shall consider only the cases that exclude the steps that do not change the pattern configuration. Therefore, in all time steps the number of tumor cells increases or decreases by an unity with probabilities g or r, respectively. Particularly, we shall study the follwing variation of the original WB model: at each time step a cell type is chosen, either a tumor cell, with probability r, or a normal cell, with probability g. Then, the selected cell is converted to its opposite type. In other words, at each time step, either the *division* or *death* of a single tumor cell occurs, with probabilities g or r, respectively.

Now, we introduce a new model by assuming that the division and death probabilities depend on the total number of tumor cells n through *Michaelis-Mentem* functions [1]:

$$g(n) = 1 - \frac{\alpha n}{\Gamma + n} \tag{3}$$

and

$$r(n) = \frac{\alpha n}{\Gamma + n}. \tag{4}$$

Here $0 < \alpha < 1$ and $\Gamma > 0$ are parameters that control the shape of the curves. These functional forms were used because they are the simplest ones which varies monotonically with n and satisfy the normalization condition $g(n) + r(n) = 1$. These curves are illustrated in figure 1.

3 Analysis of WB models using stochastic methods

The stochastic growth rules used in the WB models involve probabilities g and r that are explicitly time independent. In consequence, as is the case for Markov chains, the chance of these models generate a given pattern in a certain time depends only on the probabilities associated to the configurations at the previous time. So, the WB growth processes will be described within the *probability transition equation* or *master equation* frameworks, according to the discrete or continuous character of the time [3,10].

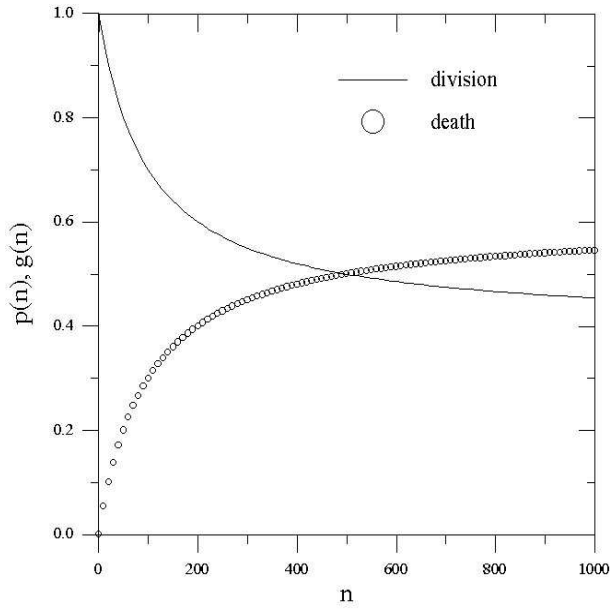

Fig. 1. Division and death probabilities in the extend WB model.

The transition probability equation is written as:

$$P(n, t+1) = \sum_m T_{n,m} P(m, t), \tag{5}$$

where $T_{m,n}$ are the elements of the *transition matrix*. $T_{m,n}$ provides the transition probability from a state containing m tumor cells to a state with n tumor cells in the next time. A continuous version of equation (5) is given by the master equation:

$$\frac{d}{dt} P(n, t) = \sum_{m \neq n} \left\{ W_{n,m} P(m, t) - W_{m,n} P(n, t) \right\}, \tag{6}$$

where $W_{n,m}$ is interpreted as a probability by unit time or transition rate.

Initially, the discrete time WB model will be considered. At every random selection of an interfacial site to implement an action, the time is incremented by an unity. In this way, the transition matrix is:

$$T_{n,m} = \begin{cases} g \text{ if } n = m + 1 \\ r \text{ if } n = m - 1 \\ 0 \text{ if } |n - m| > 1 \end{cases} . \tag{7}$$

This expression is valid only for $n \geq 2$, since the WB model is a special type of *one step process* [3] with an absorbent state at $n = 0$. Indeed, $T_{0,1} = r$ and

$T_{1,0} = 0$. Substituting the transition matrix (7) in the probability transition equation (5) we have:

$$\begin{aligned} P(n,t+1) &= gP(n-1,t) + rP(n+1,t) \text{ if } n \geq 2 \\ P(n,t+1) &= rP(n+1,t) \qquad\qquad\qquad\quad \text{if } n = 0,1 \end{aligned} . \tag{8}$$

In this section, we are interested in quantities that depend only on the number of tumor cells and not on the spatial distribution of theses cells on the tissue. So, the time dependence of the average number of tumor cells $\langle n(t) \rangle$ and its variance $\sigma(t)$, defined as:

$$\langle n(t) \rangle \equiv \sum_{n=0}^{\infty} nP(n,t) \tag{9}$$

and

$$\sigma^2(t) \equiv \langle n^2(t) \rangle - \langle n(t) \rangle^2, \tag{10}$$

are calculated. Clearly,

$$\langle n^2(t) \rangle \equiv \sum_{n=0}^{\infty} n^2 P(n,t). \tag{11}$$

Using equation (8) and iterating the expressions for $< n(t) >$ and $< n^2(t) >$ we find:

$$\langle n(t) \rangle = n(0) + \frac{\kappa - 1}{\kappa + 1} t \tag{12}$$

and

$$\sigma^2(t) = \left[1 - \left(\frac{\kappa - 1}{\kappa + 1} \right)^2 \right] t. \tag{13}$$

Equations (12) and (13) show that $\langle n(t) \rangle$ decreases linearly with time if $\kappa < 1$, and increases linearly if $\kappa > 1$. In turn, the variance increases with the square root of time. Thus, for all $\kappa > 1$ there is a non-vanishing probability of unlimited tumor growth. But, if $\kappa = 1$, $\langle n(t) \rangle$ is constant, the variance increases with the square root of time and, therefore, independently of the initial population, the absorbent state $n = 0$ will be reached. Moreover, we have the maximum variance exactly at $\kappa = 1$. These exact results found for the discrete WB model are also valid for the continuous time approach.

4 The extended model

In this section, the previously described generalized WB model (equations (3) and (4)), which includes the possibility of growth limitation, is studied by a continuous approach based on the master equation [3,10]. Again, the time step is defined as the birth or death of a single tumor cell.

4.1 The macroscopic equation

First of all, we define the transfer matrix $W_{n,m}$:

$$W_{n,m} = \begin{cases} g(m) \text{ if } n = m + 1 \\ r(m) \text{ if } n = m - 1 \\ 0 \text{ if } |n - m| > 1 \end{cases} \tag{14}$$

or

$$W_{n,m} = g(m)\delta(m - n - 1) + r(m)\delta(m - n + 1). \tag{15}$$

The master equation is obtained substituting the expression (15) in (6):

$$\frac{d}{dt}P(n,t) = g(n-1)P(n-1,t) + r(n+1) \times P(n+1,t) - P(n,t). \tag{16}$$

Using (9), (11) and (16) we have:

$$\frac{d\langle n(t)\rangle}{dt} = 1 - 2\alpha \left\langle \frac{n(t)}{\Gamma + n(t)} \right\rangle \tag{17}$$

and

$$\frac{d\langle n^2(t)\rangle}{dt} = 1 + 2 \left\langle \frac{n(t)[\Gamma + (1-2\alpha)n(t)]}{\Gamma + n(t)} \right\rangle. \tag{18}$$

Notice that (17) and (18) are non-linear equations which cannot be solved by analytical or numerical methods. Using a mean field approximation, the macroscopic equation for (17) is obtained replacing $n(t)$ by a deterministic

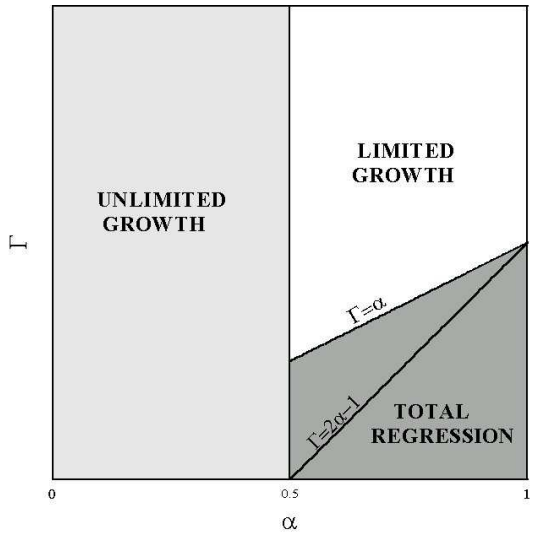

Fig. 2. Mean field phase diagram for the asymptotical value of the average number of tumor cells. Three possible regimes are found: unrestricted growth, limited growth and total regression of the tumor.

function $N(t)$. The corresponding macroscopic equations for the first and second moments are:

$$\frac{dN(t)}{dt} \equiv \zeta(t) = 1 - 2\alpha \frac{N(t)}{\Gamma + N(t)}. \tag{19}$$

$$\frac{dN_*^2(t)}{dt} = 1 + 2\frac{N(t)[\Gamma + (1-2\alpha)N(t)]}{\Gamma + N(t)}. \tag{20}$$

The star is used in order to distinguish between N^2 and N_*^2, the second moment.

As one can see, equation (19) exhibits three distinct asymptotic behaviors:

- $N(t)$ increases without limit if $\zeta(t) > 0 \ \ \forall \ \ t$;
- $N(t) \to 0$ if $\zeta(t) < 0 \ \ \forall \ \ t$;
- $N(t)$ goes to a non-vanishing constant value if $\zeta(t) = 0$ at a certain time.

The phase diagram in the parameter space (Γ, α) is shown in figure 2. The third behavior requires a stable solution [3], which always exists since the macroscopic equation is a first order differential equation. This analysis reveals the existence of a well-defined phase transition in $\alpha = 1/2$, i. e., for $\alpha < 1/2$ the average number of tumor cells grows without limit, whereas for $\alpha > 1/2$ this number reaches a constant value $\Omega \geq 0$.

In the region of unrestricted growth ($\alpha < 1/2$), $N(t)$ grows linearly and the variance increases as the square root of the time, in agreement with (19) and (20) for very large N. Therefore, the model behaves asymptotically as

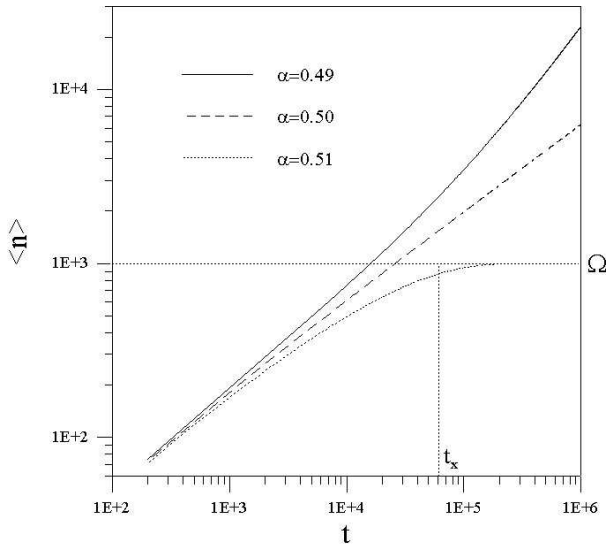

Fig. 3. Numerical solutions of the macroscopic equation for the extended WB model around the critical point $\alpha = 1/2$ and fixed parameter $\Gamma = 20$. Also, the saturation value and the crossover time evaluated for these parameters are indicated.

the original WB model. The transition line $\alpha = 1/2$ must be considered in separated. Fortunately, the equation (19) has a closed solution for $\alpha = 1/2$, $N_{\frac{1}{2}}(t)$, given by:

$$N_{\frac{1}{2}}(t) = \sqrt{(n(0) + \Gamma)^2 + 2\Gamma t} - \Gamma. \tag{21}$$

Clearly, $N_{\frac{1}{2}}$ has the asymptotical behavior $N_{\frac{1}{2}}(t) \cong \sqrt{2\Gamma t}$. Substituting (21) in (20), the asymptotical macroscopic approximation to N_*^2 is obtained and, using this result, we find $\sigma = \sqrt{t}$. However, numerical simulations suggest that $\sigma \cong \sqrt{t/2}$, and this difference will be explained in the subsection 4.3 by taking into account corrections to the macroscopic equation.

In the region of limited growth, the solution $N_s(t)$ reaches a *saturation value* Ω for long times. This value can be find by taking $\zeta(t) = 0$:

$$\Omega = \frac{\Gamma}{2\alpha - 1}. \tag{22}$$

Also, the *saturation crossover time*, $(t_\times)$, is evaluated through an expansion at long times of $N_s(t)$ around Ω. Substituting $N_s(t) = \Omega + \mu(t)$, where $|\mu(t)| \ll \Omega$, and expanding (19) we have:

$$\frac{d\mu}{dt} = -\frac{(2\alpha - 1)^2}{2\alpha\Gamma}\mu + O(\mu^2). \tag{23}$$

At first order in μ the solution is an exponential decay $\mu(t) \sim \exp(-t/t_\times)$. Thus, the saturation crossover time is given by:

$$t_\times = \frac{2\alpha\Gamma}{(2\alpha-1)^2}. \tag{24}$$

In figure 3 the numerical integrations of (19) around the critical parameter $\alpha = 1/2$ and fixed $\Gamma = 20$ are shown.

The phase diagram exhibits two lines in the complete regression region. The line $\Gamma = 2\alpha - 1$ is the border of the region where $N(t) \to 0$, according to the solution of the macroscopic equation. However, if the fluctuations are larger than the saturation value Ω, all tumor cells die. Thus, the phase diagram shown in figure 2 already take into account the correction considering the variance, as evaluated in next subsection. The result is that the region of total regression correspond to $\Gamma < \alpha$.

In order to test the predictions of the macroscopic equation approximation, comparisons with simulational results were done. It was observed a good agreement between analytical and simulational results for $\alpha < 1/2$. However, for $\alpha \geq 1/2$, small differences, that become meaningful when the value of Γ is not large, emerge. All these comparisons are shown in figure 4. As one can see, there is a fixed difference between the numerical and simulated solutions in the limited growth region. This difference can be found making an *expansion of the master equation* [3], also called Ω *expansion.*

4.2 The Ω expansion

The Ω expansion consists in expand the master equation in powers of the characteristic size of the system. In our case, this characteristic size is the Ω in (22), since it represents an upper bound to the size of the tumor population. Indeed, this was the reason for denote the saturation value as Ω.

We assume that the probabilities P_n have a sharp maximum around the macroscopic solution with a width of order $\Omega^{1/2}$. This hypothesis is explicitly used in the change of variable:

$$n = \Omega\phi(t) + \Omega^{1/2}\xi, \tag{25}$$

where ξ is a new random variable and $\phi(t)$ is a deterministic function. Also, the expansion assumes that the rates $W(n|m) \equiv W_{n,m}$ can be written in the

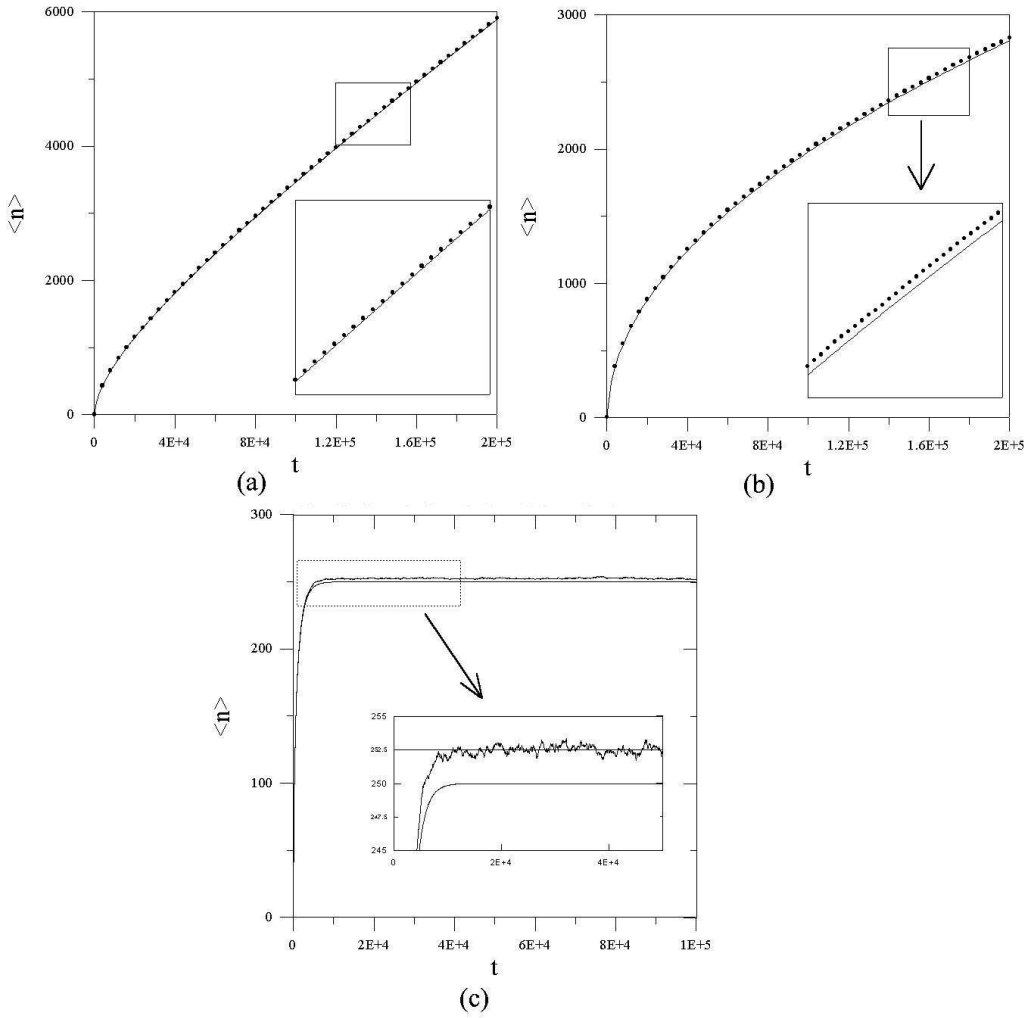

Fig. 4. Comparison between analytical and simulational results. The continuous and smooth curves are obtained from numerical integrations of the macroscopic equation whereas the other ones are given by simulations. 2000 samples were used in the simulations with the parameters (a) $\Gamma = 20$ and $\alpha = 0.49$, (b)$\Gamma = 20$ and $\alpha = 1/2$ and (c) $\Gamma = 50$ and $\alpha = 0.60$.

form:

$$W_\Omega(n|m) = f(\Omega)\left\{\Phi_0\left(\frac{m}{\Omega};s\right) + \Omega^{-1}\Phi_1\left(\frac{m}{\Omega};s\right) + \Omega^{-2}\Phi_2\left(\frac{m}{\Omega};s\right) + \ldots\right\}, \quad (26)$$

where f and Φ_i are arbitrary functions and $s \equiv n - m$. The technical details involved in the expansion can be found in [3].

Introducing the notation used in [3]:

$$\varphi_{\nu,\lambda}(x) = \int s^\nu \Phi_\lambda(x;s)ds, \quad (27)$$

the expansion up to orders of $\Omega^{1/2}$ and Ω^0 results in the following equations for ϕ, $\langle\xi\rangle$ and $\langle\xi^2\rangle$:

$$\frac{d\phi}{d\tau} = \varphi_{1,0}(\phi), \tag{28}$$

$$\frac{\partial\langle\xi\rangle}{\partial\tau} = \varphi'_{1,0}(\phi)\langle\xi\rangle \tag{29}$$

and

$$\frac{\partial\langle\xi^2\rangle}{\partial\tau} = 2\varphi'_{1,0}(\phi)\langle\xi^2\rangle + \varphi_{2,0}(\phi), \tag{30}$$

with $\tau \equiv f(\Omega)/\Omega$. (28) is the macroscopic equation for the system divided by Ω, (29) gives the correction for $\langle n(t)\rangle$ in order of $\Omega^{1/2}$, and (30) represents the first approximation for the fluctuations around the mean. The initial conditions for (29) and (30) are $\langle\xi(0)\rangle = \langle\xi^2(0)\rangle = 0$, because $P_n(0) = \delta(n - n_0)$, i.e., at $t = 0$ the population is n_0.

For the extended model, the transition rates (15) can be rewritten as:

$$W_\Omega(\rho; s) = \left(1 - \frac{\alpha\rho}{2\alpha - 1 + \rho}\right)\delta(s-1) + \left(\frac{\alpha\rho}{2\alpha - 1 + \rho}\right)\delta(s+1), \tag{31}$$

where $\rho \equiv m/\Omega$. In agreement with the notation of (26), we have $f(\Omega) = 1$, $\Phi_i = 0$ if $i \neq 0$, and Φ_0 is defined as the right hand side of (31).

Here, our goal is calculate the asymptotical corrections in time and the differences shown in figure 4. Solving (29) and (30) using (31), we find that:

$$\langle\xi(\tau)\rangle \sim \exp\left(-\frac{2\alpha - 1}{2\alpha}\tau\right) \overset{\tau\to\infty}{\longrightarrow} 0 \tag{32}$$

and

$$\langle\xi^2(\tau)\rangle \overset{\tau\to\infty}{\longrightarrow} \frac{\alpha}{2\alpha - 1}. \tag{33}$$

Therefore, the correction for $\langle n(\infty)\rangle$ given by (32) vanishes, because $n = \Omega\phi(t) + \Omega^{1/2}\xi(t)$. However, (33) shows that the first correction for the variance reaches a constant value:

$$\sigma^2 = \Omega\langle\xi^2(\tau)\rangle \overset{\tau\to\infty}{\longrightarrow} \frac{\Gamma\alpha}{(2\alpha - 1)^2}. \tag{34}$$

In figure 4(c) the variance was measured as $\sigma_{measured} \cong 27.5$, whereas the analytical value calculated by (34) is $\sigma_{analytical} \cong 27.4$. Thus, there is an excellent agreement between the analytical and simulational results for the variance. Since the fluctuations reach a constant value which is smaller than the saturation one, the tumor certainly does not disappear as in the original WB model with $\kappa = 1$.

The difference between the saturation values obtained by the simulations and calculated through the macroscopic equation can not be explained taking into account only terms of order Ω^0. The first non-vanishing correction in $\langle\xi\rangle$ involves terms of order $\Omega^{-1/2}$[3]:

$$\langle\xi\rangle = \frac{\Omega^{-1/2}}{2(2\alpha - 1)}. \tag{35}$$

Consequently, the first correction in $\langle n\rangle$ is:

$$\Delta = \frac{1}{2(2\alpha - 1)}. \tag{36}$$

Using (36), the calculated correction is $\Delta_{analytical} = 2.5$ and the measured value in figure 4(c) is $\Delta_{measured} \cong 2.51$, which are in excellent agreement. Several other values for the model parameters were tested and a very good agreement between simulational and analytical results was found.

4.3 Asymptotical corrections for $\alpha = 1/2$

The Ω expansion cannot be applied for systems without a characteristic size. This is the case for equation (21) which, for $\alpha = 1/2$, gives a solution that grows without limit and, consequently, one can not define the characteristic size of the tumor. However, it is possible to do an expansion around the macroscopic solution (21). Taking $n(t) = N_{\frac{1}{2}}(t) + \varepsilon(t)$, where ε is the new random variable satisfying $|\varepsilon(t)|/N_{\frac{1}{2}}(t) \ll 1$, and conserving terms up to second order of $\varepsilon/N_{\frac{1}{2}}$, we find the following equation for $\varepsilon(t)$:

$$\frac{d < \varepsilon >}{dt} = -\Gamma\frac{< \varepsilon >}{g^2(t)} + \Gamma\frac{< \varepsilon^2 >}{g^3(t)} + O(\varepsilon^3), \tag{37}$$

where $g(t) = \sqrt{n(0) + 2\Gamma t}$. In order to solve (37), it is necessary to know the relationship between the first and the second moments of ε. Equation (20) gives $N_*^2(t) = N_{\frac{1}{2}}^2(t) + t$ and the xpansion of $n^2 = (N_{\frac{1}{2}} + \varepsilon)^2$ with the approximation $<$

$n^2 > \approx N_*^2$ results in $< \varepsilon^2 > \approx t - 2N_{\frac{1}{2}} < \varepsilon >$. Substituting this approximated relation for $< \varepsilon^2 >$ in equation (37), and taking the asymptotical limit for t, we obtain:

$$\frac{d < \varepsilon >}{dt} + \frac{3}{2t} < \varepsilon > - \frac{1}{2\sqrt{2\Gamma t}} = 0. \tag{38}$$

Its exact solution is:

$$< \varepsilon(t) > = \sqrt{\frac{t}{32\Gamma}}. \tag{39}$$

Considering the correction given by (39), the analytical and simulational curves in figure 4(b) become indistinguishable. Now, one can use the result (39) to find the correction to the variance. It is possible to show that the asymptotical value of the variance, consistent with the approximations used above, is given by:

$$\sigma^2 = \frac{t}{2}\left(1 - \frac{1}{16\Gamma}\right) \tag{40}$$

Equation (40) is able to explain the factor 1/2 present at the simulations shown in figure 4(b). Again, the simulational and analytical results are in very good agreement for a large number of parameter sets.

5 Geometrical patterns

The previous sections were dedicated to the analytical study of the original WB model and its extended version. Now, in this section the simulational results focusing the geometrical properties of the patterns generated by the extended WB model are presented. The patterns associated to the original WB model are spherical and compact with a rough surface. For the extended model, the patterns exhibit three distinct morphologies: compact with a rough border, connected with internal holes and disconnected with cells isolated from each other. These morphologies are shown in figure 5. In the region of unlimited growth, i. e., $\alpha < 1/2$, the patterns become compact. This compaction occurs because the division probability is always higher than the death probability and, as a consequence, all the internal empty sites will be occupied at sufficiently long time. The disconnected patterns appear in the region of limited growth ($\alpha > 1/2$). The reason is that the division and death probabilities reach the same value $p = 1/2$, and the cells behave like non-directed random walkers. Finally, the connected patterns are generated just on the transition

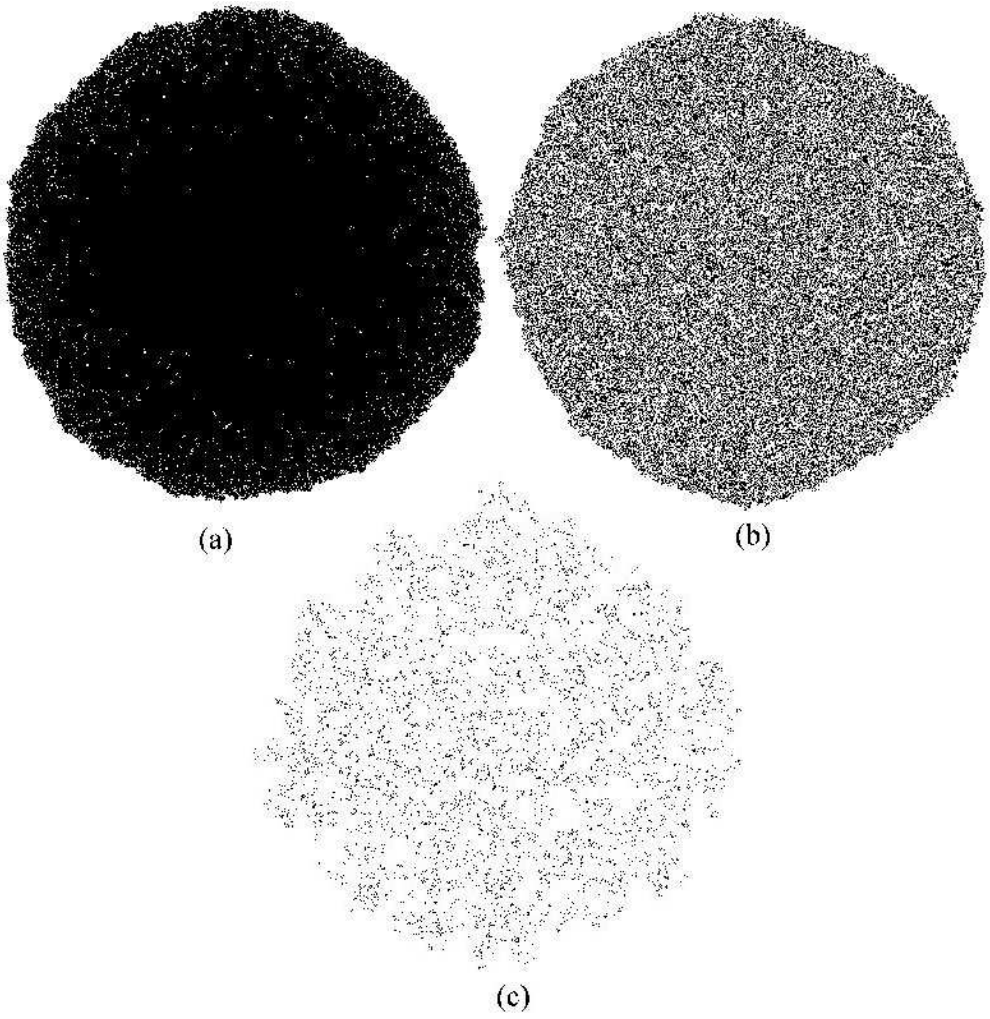

Fig. 5. Typical patterns generated by the extended WB model: (a) compact, (b) connected and (c) disconnected. For these patterns $\Gamma = 1000$ were used. $\alpha = 0.45$, 0.50 and 0.51 was used in (a), (b) and (c), respectively. The simulations were done in lattices with 1200×1200 sites and stopped if a tumor cell reaches the border of the lattice.

line $\alpha = 1/2$. The difference between connected and disconnected patterns is that the former does not has a percolation cluster of empty sites inside the pattern, whereas in the last this cluster is found.

These patterns were characterized by its gyration radius (R_g) and the number of interface tumor cells (S). The gyration radius is defined by:

$$R_g = \sum_{i=1}^{n} (\vec{r_i} - \vec{r}_{cm})^2, \tag{41}$$

where the sum extends over all the tumor cells and $\vec{r}_{cm}$ is the mass center of the pattern. In the original WB model, R_g and S scale asymptotically

Table 1
Summary of the exponents found for the extended WB model. The exponents ν, σ, and γ are defined by $R_g \sim n^{\nu}$,$S \sim n^{\sigma}$ and $\rho \sim t^{\gamma}$.

	$\alpha < 1/2$		$\alpha = 1/2$			$\alpha = 0.51$		
Γ	ν	σ	ν	σ	γ	ν	σ	γ
10^3	0.50	0.50	0.64	1	0.18	0.62	1	0.64
10^3	0.50	0.50	0.60	1	0.18	0.60	1	0.64
10^4	0.50	0.50	0.54	1	0.25	0.52	1	0.63

with the square root of the number of tumor cells [11]. In turn, only the compact patterns ($\alpha < 0.5$) of the extended model show the same asymptotical behaviour for R_g and S. For $\alpha \geq 0.5$ the scaling laws change and are dependent on the Γ parameter. Indeed, $S \sim n$ and $R_g \sim n^{\nu}$, with $\nu(\Gamma) > 1/2$, indicating that the patterns are fractals with dimensions $d_f = 1/\nu$ [8]. Notice that, in the limited growth regime, n is bounded and the power law is defined before the growth saturation. However, since the cells become progessively more distant from each other, R_g grows continuously with the time as a power law. The numerical results are summarized in table 1.

The transition from compact to disconnected patterns was studied through the density ρ of internal holes in the patterns. ρ was defined as the ratio between the number of empty and occupied sites enclosed by a circle of radius R_g. This definition was used in order to discard the tumor border, where the compaction never occurs. For $\alpha < 1/2$, ρ decreases, vanishing at sufficient long time. In contrast, for $\alpha \geq 1/2$, ρ increases asymptocally as a power law $\rho \sim t^{\gamma}$.

In order to test if the exponent γ varies with the parameter Γ, simulations were done using three distincts Γ values (10^2,10^3,10^4). For $\Gamma = 10^4$ the density of internal holes is lower than that for $\Gamma = 10^3$, but the corresponding power law exponent is higher. Since for both $\Gamma = 10^2$ and $\Gamma = 10^3$ the simulations provide essentially the same values for γ, we suppose that this exponent is independent of the parameter Γ. Thus, we believe that the curve obtained for $\Gamma = 10^4$ might be a transient behavior.

The patterns observed in the extended model are very similar to the morphologies generated by a growth model for primary cancer recently proposed [12]. This model considers a complex interaction network among tumor cells mediated by growth factors and, in contrast to the present model, involves a large number of parameters. Our results are more robust than those observed in [12], since the two parameters used in the extended WB model are not associated to the properties of the tumor microenvironment. Indeed, they are related to macroscopic quantities such as the saturation size of the tumor. However, the extended WB model has a limitation. Every compact pattern has a unlimited growth and the disconnected patterns always cease their pop-

ulational growth. The reason is that the growth only occurs on the interface between tumor and normal tissues, whereas in real tumors the internal cells also divide. This limitation does not compromise the analytical results since the spatial distribution of the tumor cells in the tissue is not considered.

6 Conclusions

In this work we propose an extended version of the Williams and Bjerknes (WB) model initially used to describe the tumor growth. In this extended model, the division and death probabilities correspond to monotonically increasing and decreasing functions of total number of tumor cells n, respectively. The average values of n for the original and the extended WB models as well as their variances were exactly calculated using stochastic processes methods. The original model reveals two possibilities for $< n >$: unlimited growth or total regression of the tumor. However, real tumors exhibit three possible behaviors which are observed also in the extended WB model: the ones previously described and a quiescent state where the tumor size remains constant for a long time. The differences observed between simulated and mean-field results for the extended model were calculated using expansions of the involved equations. In addition, the geometry of the growth patterns generated by the extended WB model were analysed. Three distinct morphologies have been observed: compact, connected and disconnected. All the patterns were characterized by its gyration radius, R_g, and number of tumor cells on the interface, S. For the compact patterns, $R_g \sim \sqrt{n}$ and $S \sim \sqrt{n}$. For the connected and disconnected patterns $R_g \sim n^{\nu}$ and $S \sim n$, with $\nu > 1/2$, indicating that these patterns are fractals.

Acknowledgements

We wish to thank Professor Ronald Dickman (Derpartamento de Física, UFMG, Brazil) and Professor M. L. Martins (Departamento de Física, UFV, Brazil) for enlightening discussions and important suggestions to improve the manuscript. This work was supported by the CNPq-Brazilian agency.

References

[1] D. Brown, P. Rothery, Models in biology: mathematics, statistics and computing, John Wiley & Sons (1993).

[2] T. Williams, R. Bjerknes, Nature 236 (1972) 19.

[3] N. G. van Kampen, Stochastic processes in Physics and Chemestry, North∼Holand (1981).

[4] P. P. Delsanto, A. Romano, M. Scarandeli, G. P. Pescarmona, Phys. Rev. E 62 2547 (2000).

[5] M. A. J. Chaplain, in A Survey of Models for Tumor-Immune System Dynamics, edited by J. A. Adam and N. Bellomo (Birkhäuser, Boston, 1997).

[6] P. C. Nowell, Science 194 23 (1976)

[7] M. Eden, in: J. Neyman (Ed.), Proceedings of fourth Berkeley symposium on mathematical statistics and probability, Vol. IV: Biology and problems of health, University of California Press, Berkeley (1961) pp. 223.

[8] T. Vicsek, Fractal Growth Phenomena, World Singapore (1992).

[9] M. T. Batchelor, B. I. Henry, S. D. Watt, Physica A 256 (1998) 295.

[10] C. W. Gardiner, Handbook of stochastic methods for Physics, Chemistry and natural sciences, Springer-Verlag (1983).

[11] S. C. Ferreira Junior, M. L. Martins, and M. J. Vilela, Physica A 261 (1998) 569

[12] S. C. Ferreira Junior, M. L. Martins, and M. J. Vilela, Physica A 272 (1999) 245